

Low temperature SCR of NO with NH₃ over carbon nanotubes supported vanadium oxides

Bichun Huang^{*}, Rong Huang, Dongjie Jin, Daiqi Ye

College of Environmental Science and Engineering, South China University of Technology, Guangzhou 510640, PR China

Available online 16 July 2007

Abstract

A novel multiwalled carbon nanotube (CNTs) supported vanadium catalyst was prepared. The structure of catalyst prepared was characterized by TEM, BET, FTIR, XRD and temperature-programmed desorption (TPD) methods. The results indicated that vanadium particles were highly dispersed on the wall of carbon nanotubes. The V₂O₅/CNT catalysts showed good activities in the SCR of NO with a temperature range of 373–523 K. The Lewis acid sites on the surface of V₂O₅/CNT are the active sites for the selective catalytic reduction (SCR) of NO with NH₃ at low temperatures. It was suggested that the reaction path might involve the adsorbed NH₃ species reacted with NO from gaseous phase and as well as the adsorbed NO₂ species. The diameter of CNTs showed positive effect on the activities of the catalysts. Under the reaction conditions of 463 K, 0.1 Mpa, NH₃/NO = 1, GHSV = 35,000 h^{−1}, and V₂O₅ loading of 2.35 wt%, the outer diameter of CNTs of 60–100 nm, the NO conversion was 92%.

© 2007 Elsevier B.V. All rights reserved.

Keywords: Low temperature SCR; Vanadium catalyst; Carbon nanotubes; NO

1. Introduction

The selective catalytic reduction (SCR) of NO with NH₃ in the presence of excess oxygen has been well proven and performed at a commercial scale in the removal of NO_x from stationary sources [1,2]. The SCR catalyst used in industrial practice is based on TiO₂, with vanadium oxide as the catalytic active phase. WO₃ or MoO₃ have been reported to be used as promoters [1,3]. The operation temperature of the catalyst is between 300 and 400 °C. So, the SCR unit has to be placed in the upstream of the desulfurizer and electrostatic precipitators for the high temperature of the flue gas. However, the high concentration of particles and SO₂ content in the flue gas reduce the performance and life of the catalyst monoliths [4,5]. Therefore, there is a great interest in developing new catalysts which are active at relatively low temperatures (<200 °C), which is the typical temperature of flue gases in the downstream. Various catalysts have been found with high activities at low temperature [4–16]. Among the reported catalysts, metal oxides (V, Fe, Mn, Cu) supported on carbon

materials (AC, AFC) have shown very high activity and resistance to the remaining SO₂ [8–15]. The performance of the carbon-supported catalysts was significantly affected by the pore structure and surface properties of the supports.

As a novel carbon material, carbon nanotubes (CNTs) have attracted much attention due to their unique electric, mechanical and structural characteristics for a variety of future applications [17,18]. With the tunable pore structure and surface properties and the large specific surface area, carbon nanotubes have been regarded as the perfect supporting materials for catalysts [19,20]. In this contribution, we report V₂O₅/CNTs as a highly efficient catalyst for NO reduction with NH₃ at low temperature. Effects of reaction temperature, V₂O₅ loading and CNTs diameter on SCR activity were presented. The effect of surface properties of CNTs on the catalytic performance was discussed.

2. Experimental

2.1. Catalyst preparation and characterization

2.1.1. Support

The employed multiwalled carbon nanotubes were purchased from Shenzhen Nanopoint Company, and were prepared

^{*} Corresponding author.

E-mail address: cebhuang@scut.edu.cn (B. Huang).

by CVD method. The raw CNTs were oxidized by means of immersion in a 12 mol/l of HNO_3 solution and refluxed at boiling point for 2 h. This was to open the CNT tube and to introduce oxygenated surface groups onto the wall of CNTs. The sample was then washed with deionized water till pH 6–7, and dried at 383 K.

2.1.2. Catalysts

The supported V_2O_5 catalysts were prepared by an incipient wetness technique. The HNO_3 -treated CNTs was impregnated in an aqueous solution of VO^{2+} prepared from ammonium metavanadate and oxalic acid as described by Economidis et al. [21] at room temperature for 24 h, then dried at 383 K for 8 h and calcified at 623 K for 2 h.

2.1.3. Characterization

The specific surface area, pore volume and pore diameter of the CNTs and catalysts as prepared were analyzed by an ASAP-2010. The pore volume was calculated using the BET method. The vanadium contents of the prepared catalysts were evaluated by EDS with Oxford Inca 300. A Philips CM300 transmission electron microscope was used for TEM. FT-IR spectra were collected on a Bruker Vector 33. X-ray diffractions were carried out by a Rigaku D/max-III A X-ray Diffractometer with Cu K α radiation at a scanning rate of 12 min^{-1} .

2.2. Catalytic activity tests

The evaluation of the catalyst activity was performed in a quartz fixed-bed continuous flow reactor, operating at a pressure of 0.1 MPa. Two hundred milligram catalyst was used in each test. The gas composition was 800 ppm NO, 800 ppm NH_3 , 5 vol% O_2 balanced by He. The total flow rate was 500 ml min^{-1} , which corresponds to a space velocities (GHSV) of $35,000 \text{ h}^{-1}$. NO concentrations in the inlet and outlet gases were measured by an on-line FSI Model flue gas analyzer. N_2O and NO_2 concentrations in the outlet gases were measured continuously by a gas chromatograph with Porapak Q column.

2.3. Temperature-programmed desorption (TPD)

The temperature-programmed desorption of NH_3 , NO, and $\text{NO} + \text{O}_2$ were carried out in a quartz microreactor. Hundred milligram sample was preheated in He at 473 K for 1 h to

remove any adsorbed species. Then the sample was cooled to 323 K in He (40 ml min^{-1}) and 10% reactants (NH_3 , NO, or $\text{NO} + \text{O}_2$) balanced by He were adsorbed at this temperature at the total flow rate of 40 ml min^{-1} until no signal variation of the gas was detected. Subsequently the sample was purged with 40 ml min^{-1} of He until no reactant was detected in the outlet, and then ramped to 673 K at a linear heating rate of 4 K min^{-1} in He (40 ml min^{-1}). The analysis of the effluent gases was performed with a gas chromatograph.

3. Results and discussion

The N_2O and NO_2 have not been observed through this low temperature SCR of NO on the $\text{V}_2\text{O}_5/\text{CNT}$ catalysts. The deNOx activity was expressed as the conversion of NO to N_2 .

The surface areas, pore volumes and pore diameters (inner diameters) of the raw CNTs, HNO_3 -treated CNTs and 2.35 wt% $\text{V}_2\text{O}_5/\text{CNT}$ catalyst were listed in Table 1. The pores of the raw CNTs supports were mainly meso-pores ($>2 \text{ nm}$). Oxidation of CNTs by HNO_3 provokes a significant increasing in surface area. After impregnation, the surface area of as-prepared catalyst slightly decreased relevant to vanadium species dispersed on the surface of support. TEM shows that the HNO_3 treatment makes most of the carbon nanotubes open (Fig. 1b), which leads to an increase of the surface areas. For $\text{V}_2\text{O}_5/\text{CNT}$ catalyst, V_2O_5 particles were located on the wall of the tubes (Fig. 1c). The particle sizes of the V_2O_5 were between 6 and 12 nm. The XRD pattern (not showed) of the $\text{V}_2\text{O}_5/\text{CNT}$ catalysts with V_2O_5 loading of 0.47–2.82 wt% indicates that only the diffraction peaks corresponding to carbon were observed.

Fig. 2 illustrated FT-IR results of the raw CNTs, HNO_3 -treated CNTs and $\text{V}_2\text{O}_5/\text{CNT}$ sample. HNO_3 -treated CNTs showed adsorption peaks corresponding to stretching vibration of C=O (1724 and 1650 cm^{-1}), and stretching vibration of C–O (1392 and 1218 cm^{-1}) [22]. This indicates that oxygenated groups were created on the surface of CNTs after the HNO_3 treatment. The oxygenated surface groups were suggested to be the anchoring sites for vanadia precursor [4]. After calcinations, the adsorption peaks disappeared and vanadium particles dispersed on CNTs.

Fig. 3 shows the performance of non-impregnated CNTs (outer diameter = 20–40 nm) and $\text{V}_2\text{O}_5/\text{CNT}$ catalyst for NO reduction at the reaction temperatures of 343–573 K. NO conversion over non-impregnated CNTs drops as the

Table 1

The surface area, pore diameter and pore volume of CNTs and $\text{V}_2\text{O}_5/\text{CNT}$

Raw CNTs						HNO_3 -treated CNTs	$\text{V}_2\text{O}_5/\text{CNT}$
Outer diameter (nm)	Average inner diameter (nm)	V_{micro} ($\text{cm}^3 \text{ g}^{-1}$)	S_{BET} ($\text{m}^2 \text{ g}^{-1}$)	S_{meso} ($\text{m}^2 \text{ g}^{-1}$)	$S_{\text{meso}}/S_{\text{BET}}$ (%)	$S_{\text{BET}} \text{ m}^2 \text{ g}^{-1}$	$S_{\text{BET}} \text{ m}^2 \text{ g}^{-1}$
<10	2	0.004	271.094	260.194	96.0	379.532	368.254
10–20	5	0.009	124.300	104.700	84.2	265.151	254.400
20–40	8	0.005	95.260	82.960	86.5	123.000	105.025
40–60	10	0.009	49.900	27.500	55.1	77.561	62.049
60–100	15	0.003	33.333	18.000	54.0	66.312	56.127

V_2O_5 loading for $\text{V}_2\text{O}_5/\text{CNT}$ sample: 2.35 wt%.

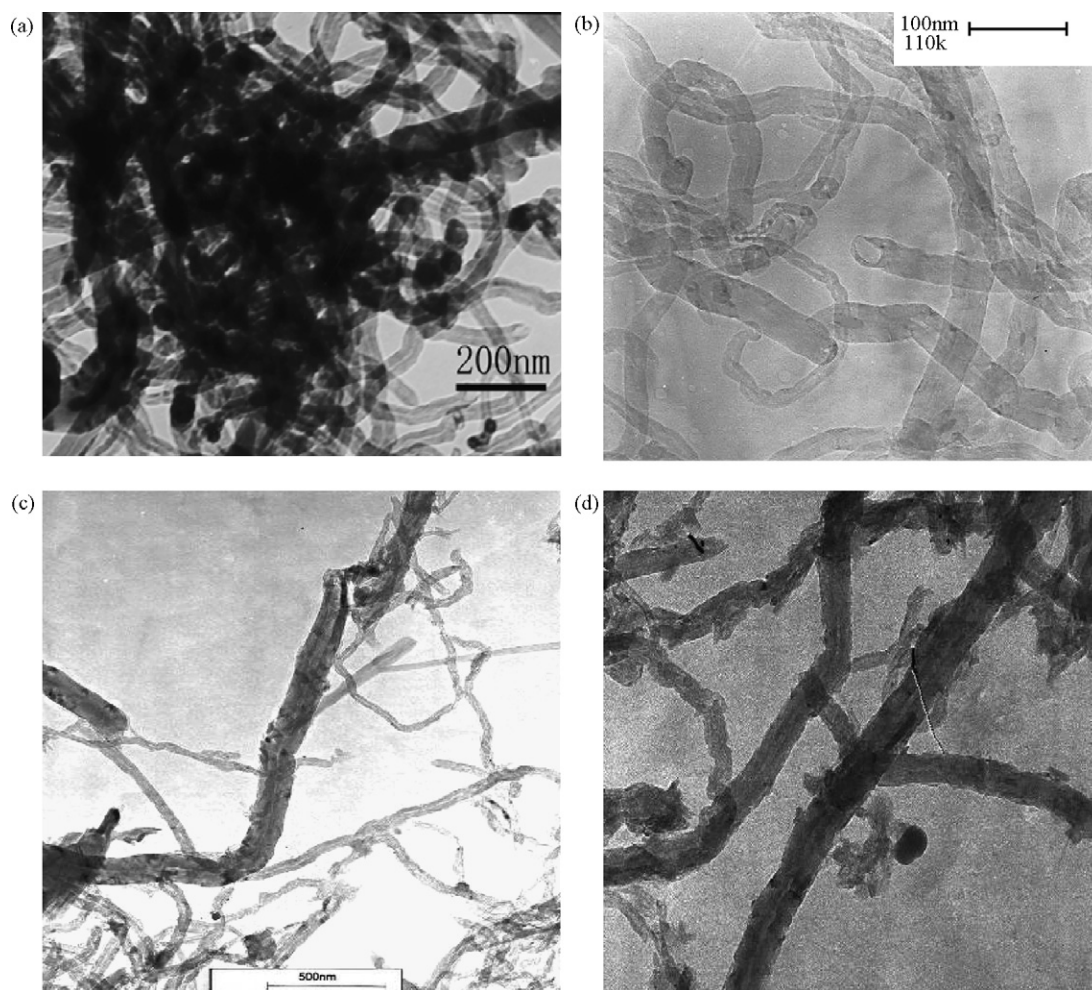


Fig. 1. TEM micrographs of (a) raw CNTs; (b) HNO_3 -treated CNTs; (c) V_2O_5 (2.35 wt%)/CNT; (d) V_2O_5 (2.82 wt%)/CNT (outer diameter of CNTs: 20–40 nm).

temperature increases. The activities of the CNTs are quite low in the whole temperature range, with NO conversions less than 6%. The NO conversion mechanism over CNTs at low temperatures is proposed by Valdes-Solis et al. [12], which

involves the physical adsorption of NO on the carbon surface. Increasing temperature causes a decrease in physical adsorption and consequently a decrease in NO removal. For the V_2O_5 /CNT catalyst, the addition of V_2O_5 leads to a significant increase in

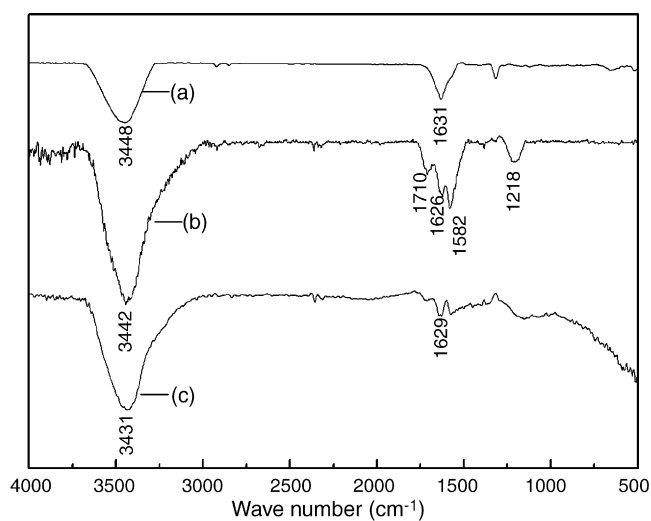


Fig. 2. FT-IR spectra of (a) raw CNTs; (b) CNTs oxidized by HNO_3 ; (c) V_2O_5 /CNT (outer diameter of CNTs: 20–40 nm, V_2O_5 loading for V_2O_5 /CNT sample: 2.35 wt%).

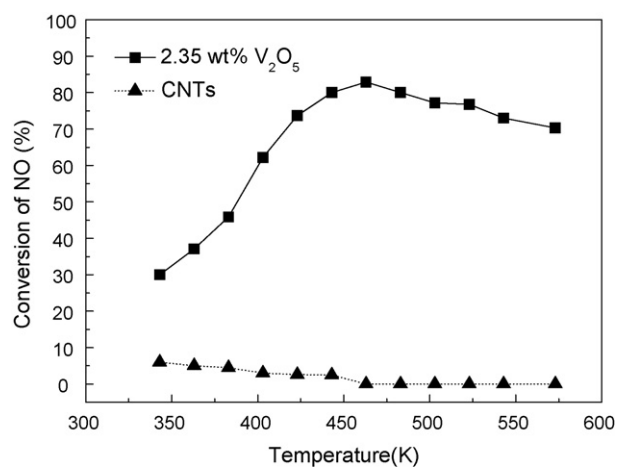


Fig. 3. Effect of reaction temperature on NO conversion (outer diameter of CNTs: 20–40 nm, V_2O_5 loading for V_2O_5 /CNT sample: 2.35 wt%; reaction conditions: GHSV = $35,000 \text{ h}^{-1}$, gas inlet: 5% O_2 , 800 ppm NO, $\text{NH}_3/\text{NO} = 1.0$).

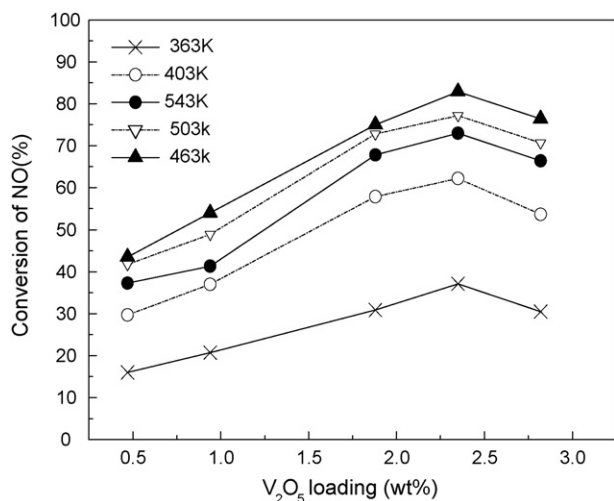


Fig. 4. Effect of V₂O₅ loading on NO conversion (outer diameter of CNTs: 20–40 nm; reaction conditions: GHSV = 35,000 h⁻¹, gas inlet: 5% O₂, 800 ppm NO, NH₃/NO = 1.0).

catalytic activity. NO conversion increases with increasing reaction temperature in the range of 343–463 K, which corresponds to an activated process. The NO conversion reaches a maximum at 463 K, and then decreases in the temperature range greater than 463 K. The decline of NO conversion over 463 K might be caused by ammonia oxidation.

Activities as a function of V₂O₅ loading is shown in Fig. 4. With increasing V₂O₅ loading from 0.47 to 2.35 wt%, NO conversion increases from 44 to 83% and then drops to 76% at a V₂O₅ loading of 2.82%. From Fig. 1(d), the agglomeration of V₂O₅ particles could be observed at V₂O₅ loading of 2.82%, which might result in the decreasing of NO conversion. At a V₂O₅ loading of 2.35 wt%, the ratio between the V₂O₅ content and the surface area was 1.08 μmol m⁻², which was lower than the monolayer coverage, which was commonly accepted to be 6–7 μmol m⁻² for vanadia [4,23].

Fig. 5 shows the effect of CNTs diameter on the catalyst activities. The activity of V₂O₅/CNT catalyst increases with

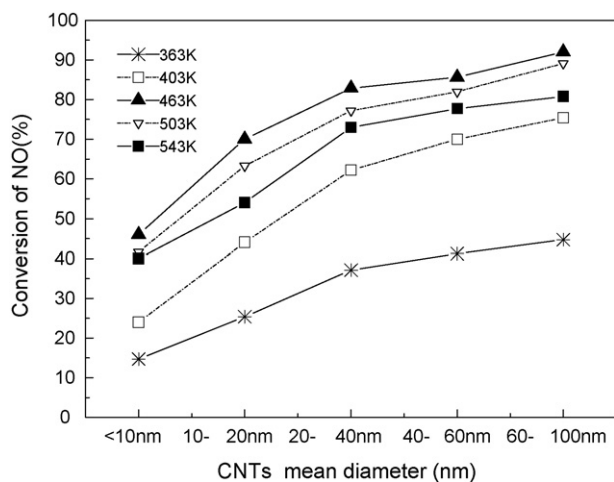


Fig. 5. Effect of CNTs mean diameter on NO conversion (V₂O₅ loading: 2.35 wt%; reaction conditions: GHSV = 35,000 h⁻¹, gas inlet: 5% O₂, 800 ppm NO, NH₃/NO = 1.0).

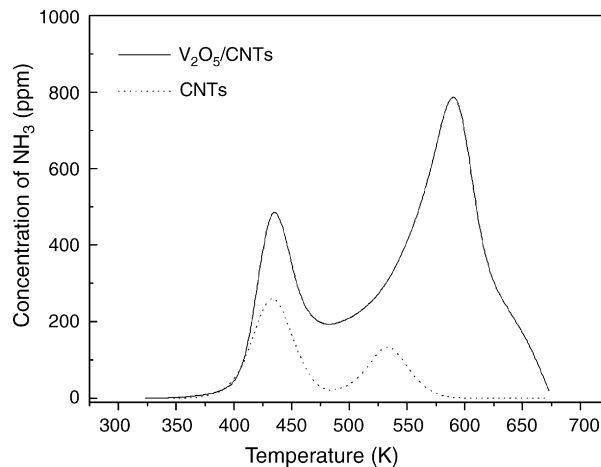


Fig. 6. NH₃-TPD spectrum of CNTs and V₂O₅/CNT (outer diameter of CNTs: 60–100 nm, V₂O₅ loading for V₂O₅/CNT sample: 2.35 wt%).

increasing CNTs diameter, which results in a NO conversion of 92% with the outer diameter of 60–100 nm. Accordingly, the V₂O₅ coverage of the catalyst was 1.99 μmol m⁻². Correlated with the data of surface areas of catalysts with different CNTs diameters (see Table 1), this indicates that the surface area was not a crucial factor for the catalytic activity in the case of V₂O₅/CNT, and a higher V₂O₅ coverage was favored for NO conversion at low temperatures. It could be associated with the available oxygenated surface groups for CNTs with different diameters in the process of HNO₃ treatment, and the dispersion of vanadium particles on the surface of CNTs.

Fig. 6 shows the temperature-programmed desorption curves recorded after NH₃ adsorption over CNTs and V₂O₅/CNT. The result indicates that there were two types of acid sites on the samples where NH₃ could be adsorbed. According to Ref. [24], it might be supposed that the low-temperature peak was mainly caused by desorption of ammonia bounded to weak Brønsted acid sites and physisorbed ammonia molecules, while high-temperature maximum could be attributed to the desorption of NH₃ from Lewis acid sites. Compared to CNTs support, vanadium species showed significant adsorption ability toward to NH₃ at Lewis acid sites. The amount of desorbed NH₃ was calculated by integration of the areas under corresponding desorption peaks (Table 2). It was apparent that the CNTs support adsorbed some ammonia but the major part of acidity was due to the vanadium species on the CNTs. Correlating with the catalytic activity of the catalysts, it could be considered that the Lewis acid sites on the vanadium species were the active sites for catalytic reduction of NO at low temperatures over V₂O₅/CNT catalyst.

It should be noticed that in the NO temperature-programmed desorption study no peak related to the desorption of NO were not observed in our study (figure not included). But with the presence of oxygen, NO and NO₂ desorption band were observed on the V₂O₅/CNT catalyst (Fig. 7). Compared to the significant adsorption ability toward to NH₃, the adsorption capacity of the catalyst towards NO and NO₂ were quite low (Table 3). It might be proposed that the reaction path of the SCR of NO with NH₃ at low temperatures over V₂O₅/CNT catalyst

Table 2
The desorption amount of NH_3 -TPD

Sample	Peak T_m (K)	Desorption amount ($\mu\text{mol/g}$)	Peak T_m (K)	Desorption amount ($\mu\text{mol/g}$)	Total desorption amount ($\mu\text{mol/g}$)	NH_3/V (mol/mol)
CNTs	433	51	533	29	81	
$\text{V}_2\text{O}_5/\text{CNT}$	435	97	589	369	466	1.8045

Outer diameter of CNTs: 60–100 nm, V_2O_5 loading for $\text{V}_2\text{O}_5/\text{CNT}$ sample: 2.35 wt%.

Table 3
The desorption amount of $(\text{NO} + \text{O}_2)$ -TPD

Sample	Adsorption gas	Peak T_m (K)	Desorption amount ($\mu\text{mol/g}$)	NO/V (mol/mol)
$\text{V}_2\text{O}_5/\text{CNT}$	$\text{NO} + \text{O}_2$	NO 445	NO_2 465	NO 49.5 NO_2 8.7

Outer diameter of CNTs: 60–100 nm, V_2O_5 loading for $\text{V}_2\text{O}_5/\text{CNT}$ sample: 2.35 wt%.

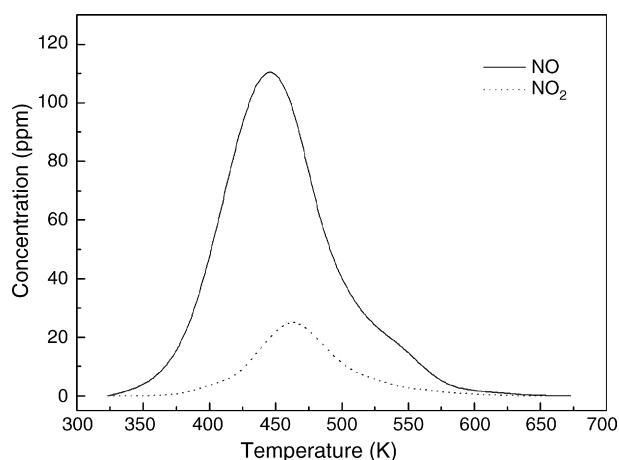


Fig. 7. $\text{NO} + \text{O}_2$ -TPD spectrum of $\text{V}_2\text{O}_5/\text{CNT}$ (outer diameter of CNTs: 60–100 nm, V_2O_5 loading: 2.35 wt%).

could be that the chemisorbed NH_3 molecules on Lewis acid sites react with NO from the gas phase and the adsorbed NO_2 species to produce N_2 and H_2O .

4. Conclusions

A new vanadium catalyst supported on carbon nanotubes for the SCR of NO with ammonia at low temperatures is reported. The prepared catalysts show a good catalytic activity at a temperature range of 373–523 K. The Lewis acid sites on the vanadium species were the active sites for the catalytic reduction of NO . It was proposed that the reaction path might involve the adsorbed NH_3 species react with NO from gaseous phase and the adsorbed NO_2 species simultaneous. The best NO conversion of 92% was obtained by using CNTs with 60–100 nm (outer diameter) as support, with a V_2O_5 loading of 2.35 wt% under the reaction conditions of 463 K, 0.1 MPa and GHSV of $35,000 \text{ h}^{-1}$.

Acknowledgements

The authors would like to gratefully acknowledge financial support from the Scientific Research Foundation for the Returned Overseas Chinese Scholars, State Education Ministry, and the Key Sci&Tec Project of Guangdong Province, China.

References

- [1] S.M. Cho, Chem. Eng. Prog. 90 (1994) 39.
- [2] H. Bosch, F.J.I.G. Janssen, Catal. Today 2 (1998) 369.
- [3] E.T.C. Vogt, M. Boot, V.A.J. Dillen, J.W. Geus, F.J.I.G. Jansen, F.M.G.V.D. Kerkhof, J. Catal. 129 (1991) 186.
- [4] E. Garcia-Bordeje, L. Calvillo, M.J. Lazaro, R. Moliner, Appl. Catal. B: Environ. 50 (2004) 235.
- [5] E. Garcia-Bordeje, M.J. Lazaro, R. Moliner, J.F. Galindo, J. Sotres, A.M. Baro, J. Catal. 223 (2004) 395.
- [6] R.Q. Long, R.T. Yang, R. Chang, Chem. Commun. 5 (2002) 452.
- [7] L. Singoredjo, R. Korver, F. Kapteijn, J.A. Moulijn, Appl. Catal. B: Environ. 1 (1992) 297.
- [8] Z. Zhu, Z. Liu, H. Niu, S. Liu, J. Catal. 187 (1999) 245.
- [9] G. Mabarn, R. Autuna, A.B. Fuertes, Appl. Catal. B: Environ. 41 (2003) 323.
- [10] G. Mabárn, T. Valdés-Solís, A.B. Fuertes, J. Catal. 226 (2004) 138.
- [11] J. Muniz, G. Maban, A.B. Fuertes, Appl. Catal. B: Environ. 27 (2000) 27.
- [12] T. Valdes-Solis, G. Marban, A.B. Fuertes, Catal. Today 69 (2001) 259.
- [13] T. Valdes-Solis, G. Marban, A.B. Fuertes, Appl. Catal. B: Environ. 46 (2003) 261.
- [14] M. Yoshikawa, A. Yasutake, I. Mochida, Appl. Catal. A: Gen. 173 (1998) 239.
- [15] Z. Zhu, Z. Liu, S. Liu, H. Niu, Appl. Catal. B: Environ. 23 (1999) L229.
- [16] S. Suárez, J.A. Martín, M. Yates, P. Avila, J. Blanco, J. Catal. 229 (2005) 227.
- [17] N.M. Rodriguez, K. Soo, R. Terry, J. Phys. Chem. 98 (1994) 13108.
- [18] J.M. Planeix, N. Coustel, B. Coq, J. Am. Chem. Soc. 116 (1994) 7935.
- [19] A. Zhang, J. Dong, Q. Xu, Catal. Today 93–95 (2004) 347.
- [20] Z. Liu, Z. Xu, W. Zhou, Phys. Chem. Chem. Phys. 3 (2001) 2518.
- [21] N.V. Economidis, D.A. Pena, P.G. Smirniotis, Appl. Catal. B: Environ. 23 (1999) 123.
- [22] L. Jiang, L. Gao, Carbon 41 (2003) 2923.
- [23] B.M. Weckhusen, D.E. Keller, Catal. Today 78 (2003) 25.
- [24] M. Niwa, Y. Habuta, K. Okumura, N. Katada, Catal. Today 87 (2003) 213.